Available online at www.sciencedirect.com

ScienceDirect

Procedia Manufacturing 13 (2017) 132–138

Procedia MANUFACTURING

www.elsevier.com/locate/procedia

Manufacturing Engineering Society International Conference 2017, MESIC 2017, 28-30 June 2017, Vigo (Pontevedra), Spain

Numerical explicit analysis of hole flanging by single-stage incremental forming

A.J. Martínez-Donaire*, D. Morales-Palma, A. Caballero, M. Borrego, G. Centeno, C. Vallellano

Dpt. Mechanical and Manufacturing Engineering, University of Seville, Camino de los Descubrimientos s/n, Seville 41092, Spain

Abstract

The use of Single-Point Incremental Forming (SPIF) technology in hole flanging operations using multi-stages strategies have been widely studied in the last few years. However, these strategies are very time-consuming, limiting its industrial application. In a very recent work of the authors, the capability of SPIF process to successfully perform hole-flanges using a single-stage strategy has been experimentally investigated. The aim of the present work is to develop a numerical model of this process to be able to predict the sheet failure as a function of the size of the pre-cut hole. The numerical results are compared and discussed in the light of experimental tests over AA7075-O metal sheets with 1.6mm thickness.

Peer-review under responsibility of the scientific committee of the Manufacturing Engineering Society International Conference 2017.

Keywords: Incremental Sheet Forming (ISF); Single-Stage; Hole Flanging; Numerical Analysis

1. Introduction

Conventional hole-flanging is a forming process used to manufacture circular or asymmetric flanges. In this process, a clamped sheet with a pre-cut hole is plastically deformed by bending and circumferential stretching with a punch. As described in [1], the magnitude of deformation in conventional circular hole-flanging can be easily characterized by the Hole Expansion Ratio (HER), which is defined as the ratio of the inside diameter d_f of the

* Corresponding author. Tel.: +34-954-487-311.
E-mail address: ajmd@us.es

2351-9789
Peer-review under responsibility of the scientific committee of the Manufacturing Engineering Society International Conference 2017.
10.1016/j.promfg.2017.09.019

finished flange to the initial hole diameter d_0. Accordingly, the formability is quantified by the Limiting Forming Ratio (LFR), i.e., the maximum HER attainable by the material (see Eq. (1)).

$$HER = \frac{d_f}{d_0} \qquad LFR := HER_{\max} = \left(\frac{d_f}{d_0} \right)_{\max} \tag{1}$$

There is a variety of parameters affecting the LFR, such as the mechanical properties of the metal sheet, the punch geometry, the punch-die clearance and others regarding the quality of the pre-cut hole edges and lubrication.

Single-point incremental forming (SPIF) is a novel technology that has been used for the last few years to obtain a variety of industrial parts due to its benefits in formability compared with conventional sheet metal forming processes [2]. In circular hole-flanging by SPIF, a flat sheet with a pre-cut hole is deformed by a forming tool that, following a pre-established trajectory using a CNC machine, progressively produces a smooth round flange. The material is now mainly deformed by a combination of circumferential and radial stretching and bending.

The use of Single-Point Incremental Forming technology in hole flanging operations using multi-stages strategies have been widely studied in the last few years [3-6]. Despite of their inherent advantages in terms of simplicity, flexibility and sustainability, these strategies are very time-consuming, so its industrial application is limited. In a very recent work, the authors experimentally investigated the capability of SPIF process to successfully perform hole-flanges using a single-stage strategy [7,8]. This version of the process allows reducing production times.

The aim of the present work is to develop a numerical model of the hole-flanging process by single-stage SPIF to analyze the material deformation and to predict the sheet failure as a function of the size of the pre-cut hole (d_0). The numerical results are compared and discussed in the light of experimental tests over AA7075-O metal sheets with 1.6mm thickness.

2. Experimentation

2.1. Setup and tools

The single-stage hole-flanging tests were carried out on a 3-axis milling CNC machine. The experimental setup consist on a blank holder and a backing plate with a 100 mm diameter hole, both fixed to the machine table through a rigid rig (see Fig. 1). The forming trajectories were modelled and simulated in CATIA V5 using the machining workbench. The step down was set to 0.2 mm per pass.

To study the deformation and failure mechanisms, the strains in the sheet surface were obtained using circle grid analysis. Specimens were previously electro-etched with a dot grid of 1 mm initial diameter and spaced by 2 mm (see circle grid in Fig. 1). The optical 3D forming analysis system ARGUS was used to automatically compute the principal strains in the sheet surface. Further details about the experimental procedure can be found in [7].

2.2. Specimens

A series of experimental tests of incremental hole-flanging by SPIF has been carried out over AA7075-O aluminum test pieces. Square sheet blanks of 170 mm side and 1.6 mm thickness with a hole milled in the center (pre-cut hole) were used. For the sake of clarity, in this work only the results of the tests with ϕ63.5 mm and ϕ65 mm pre-cut holes and a ϕ12mm hemispherical forming tool are analyzed here. As shown in Fig. 1, this pair of tests corresponds to a failed and a successful flange respectively. The inner diameter intended to achieve was always 95.8mm.

3. Numerical model

The Finite Element analysis has been performed using the ANSYS™ software, through its explicit dynamic solver LS-DYNA™.

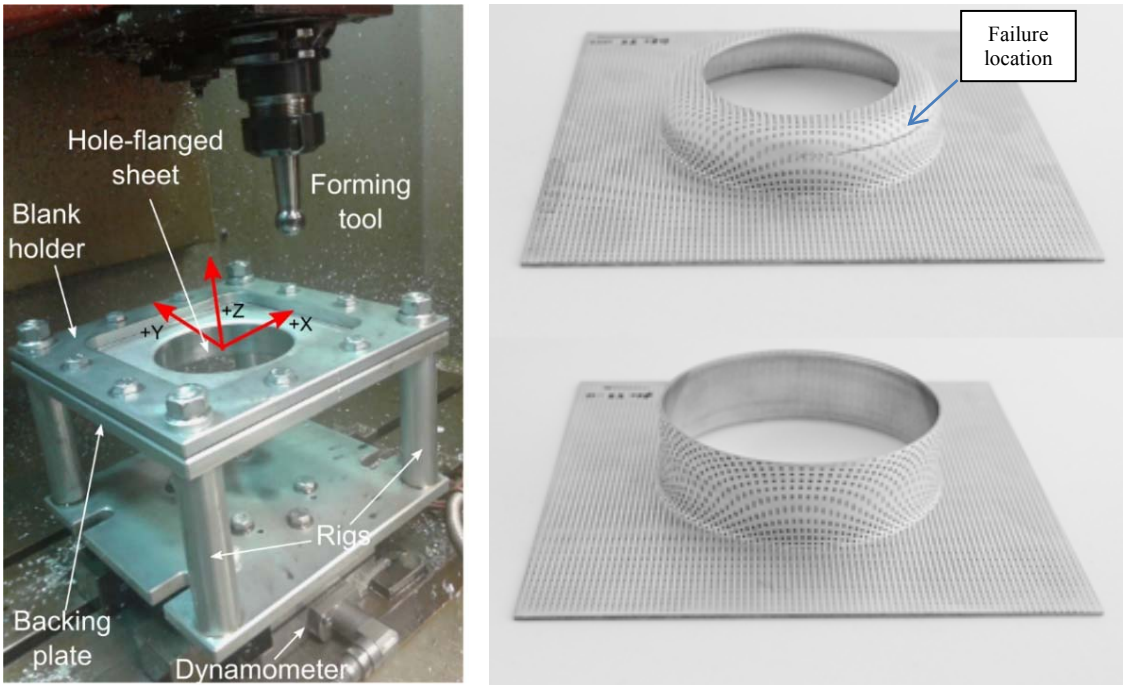

Fig. 1. Experimental setup for SPIF tests (left); Fractured flange (ϕ63.5 mm pre-cut hole) and successful flange (ϕ65 mm pre-cut hole) obtained using a ϕ12mm forming tool (right).

3.1. Finite element

A 2D element (shell type) is used for modelling of the metal sheet in order to reduce computational cost. The element available in ANSYS™ for explicit analysis is a 4 nodes element with 12 degrees of freedom on each node (SHELL163) shown in Fig. 2. The element formulation chosen is Belytschko-Tsay, as recommended for explicit dynamic analysis and forming simulations. This formulation is based on the Mindlin-Reissner theory and uses one point quadrature and hourglassing control. Five integration points along the sheet thickness are chosen in order to capture the strain gradient across the sheet thickness successfully. Finally, the backing plate and tools have been modelled as rigid bodies.

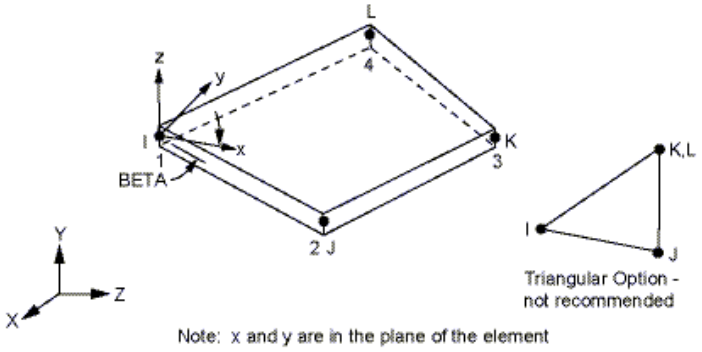

Fig. 2. SHELL163 element.

3.2. Mechanical characterization

It is assumed that metal sheet behaved as an elastic-plastic rate independent material. The elastic behavior is supposed to be isotropic. The plastic behavior is hypothesized to follow the Barlat and Lian yield criterion [9], which is highly recommended for aluminum sheets under plane stress conditions. The Barlat criterion is defined as follows:

$$2(\sigma_y)^m = a|K_1 + K_2|^m + a|K_1 - K_2|^m + c|2K_2|^m \quad (2)$$

where m is a material constant (m= 8 for aluminum alloys) and K_1 and K_2 are defined as follows:

$$K_1 = \frac{\sigma_{xx}+h\sigma_{yy}}{2} \quad ; \quad K_2 = \sqrt{\left(\frac{\sigma_{xx}-h\sigma_{yy}}{2}\right)^2 + p^2\tau_{xy}^2} \quad (3)$$

where h and p are additional anisotropy constants. These constants are evaluated by the software through the experimentally measured anisotropy ratios r_0, r_{45} and r_{90}. Table 1 summarizes the mechanical properties of the AA7075-O sheets. Further details can be found in [10,11].

Table 1. Elastic mechanical properties and anisotropy parameters for AA7075-O.

***E* (GPa)**	**ν**	r_0	r_{45}	r_{90}
65.7	0.3	0.654	0.968	0.814

A potential hardening law is selected to adjust the experimental data (see Fig. 3 (left)):

$$\bar{\sigma}(Mpa) = 255\,\bar{\varepsilon}_p^{0.06} \quad (4)$$

where $\bar{\sigma}$ is the equivalent stress and $\bar{\varepsilon}_p$ represents the equivalent plastic strain.

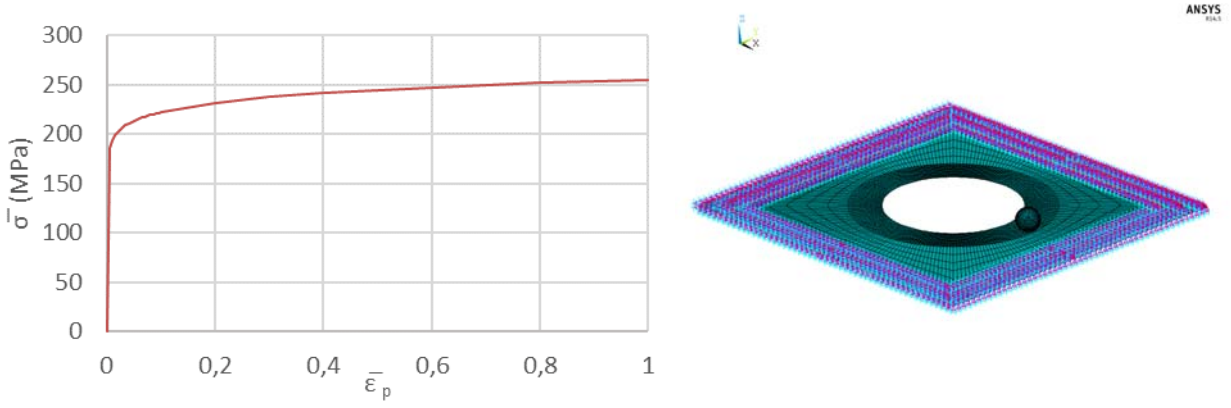

Fig. 3. Fitted hardening curve from experimental data for AA7075-O (left); Detail of the finite element mesh and boundary conditions in the blankholder region (right).

3.3. Mesh, boundary conditions and tool trajectories

The mesh size and element shape has been a balance between numerical accuracy and computational requirements. For this reason, the size of the mesh was defined finer near the pre-cut hole and coarser far from it, as shown in Fig. 3 (right).

Regarding the boundary conditions, all displacements, velocities and accelerations were prevented in the blankholder region (see Fig. 3 (right)). The static and dynamic friction factors were set to μ=0.15 both in the tool-metal sheet and backing plate-metal sheet contacts. This value was estimated from the literature for a typical aluminum-steel lubricated contact.

The trajectories followed by the tool were developed in DS CATIA V5 for ϕ12mm tool analyzed and it was the same than those used on the CNC machine. It should be highlighted that the simulated forming speed was scaled by 100, in order to reduce computational cost and calculation time. This reduction on time was also tried through mass scaling factors as typical in explicit solvers, however instability problems arisen and this option was discarded.

4. Results

Several hole-flanging operations by single stage incremental forming were simulated using ϕ12mm forming tool and several diameters of the pre-cut holes. For clarity, the results of the ϕ67.5 mm and ϕ68.5 mm pre-cut holes diameters are shown here. These simulations correspond to the numerical predictions of a failed and a successful flanged part respectively.

As can be seen in Table 2, the numerical and the experimental pre-cut holes that allow obtaining a successful flanged seems to be shifted by 4mm in diameter. This offset seems to be related to the limitations between simulated and real material behavior. For this reason, the numerical and experimental comparison should be intended as qualitative hereafter.

Table 2. Comparison between numerical and experimental results.

ϕ12mm tool		
Model	**Failure (*mm*)**	**Success (mm)**
Numerical	ϕ67.5	ϕ68.5
Experimental	ϕ63.5	ϕ65

4.1. Forming Limit Diagram (FLD) and failure prediction

Fig. 5 shows the numerical major strain contours for the last failed flange (ϕ67.5). In this one, a zone of high strains around the middle of the flange is clearly identified, indicating the fracture initiation site.

The evolution of the numerical major and minor principal strains along the flange is presented in the experimental FLD (see blue line in Fig. 5 (left)). Three different points in the flange are identified (Points a, b, and c, see Fig. 5). The Point a locates near the non-deformed zone, Point b is around the middle of the wall and Point c close to the inner edge of the pre-cut hole. The experimental evolution of principal strains measured in the last failed flange (ϕ63.5) is also shown (black dot line).

As can be seen, the shape of the numerical curves matches reasonably well with the experimental results. In the failed flanged part (Fig. 5), both numerical and experimental curves present a steep central part, reaching the experimental Fracture Forming Limit (FFL) curve and indicating successfully that failure appears at that zone. In fact, this predicted failure location agrees well with the experimental evidence, as can be seen in Fig. 1(right).

The FFL represents the experimental onset of fracture in the sheet. It should be noticed that failure by necking is not considered here as a possible failure mode. As experimentally demonstrated in [7], in current AA7075-O sheets, the SPIF process with a ϕ12 mm diameter tool yields a complete inhibition of necking during the material deformation.

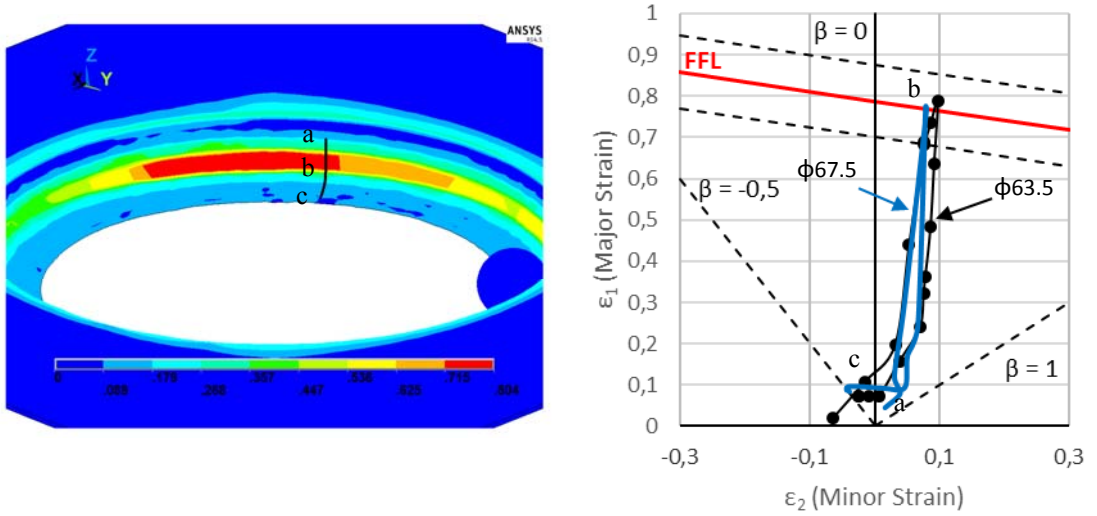

Fig. 4. Numerical results of the major principal strain contour for a failed flanged part of ϕ67.5 mm precut-hole using a ϕ12 mm tool (left); Evolutions of the principal strains in the FLD along the flange for the numerical simulation (blue line) of ϕ67.5mm precut-hole specimen and the experimental results (black dot line) for a ϕ63.5mm precut-hole specimen.

4.2. Limiting Forming Ratio (LFR)

Table 3 summarizes the results (failure or success) for the different numerical tests simulated and their experimental counterpart. The LFR (HER_{max}) obtained are also shown. As can be seen, the numerical LFR agrees reasonably well with experimental one, being in both cases around 1.4 in practice.

Table 3. Summary table of experiments and simulations

Tool diameter	Model	Pre-cut hole diameter (mm)								LFR	Flange elongation
		56	58	60	62.5	63.5	65	67.5	68.5		
12 mm	Num	X	X	X	X	X	X	X	O	1.37	32%
	Exp	X	X	X	X	X	O	O	O	1.44	43%

X= failure; O=success

As discussed in [7], LFR ratio only takes into account the maximum strain at the hole edge (circumferential strain), assuming that failure appears at this location. This is true in conventional hole flanging but not in incremental hole flanging operations. In fact, failure in incremental hole-flanging is controlled by the severe stretching and thinning in the material of the entire flange. Indeed, as mentioned before, failure is governed by the axial strain around the middle of the flange instead of only the circumferential strain near the hole edge (see Fig. 5). According to this, LFR should not be used as unique measure of formability in hole-flanging by SPIF.

A direct parameter that quantifies the axial stretching undergone by the flange is the flange height itself. The total height of the flange in the successful case is around 18 mm. Thus, in order to analyze the real forming potential, the stretching can be evaluated through the flange elongation as follows:

$$\text{Flange elongation} = \frac{l_f - l_0}{l_0} \tag{5}$$

where l_0 is the undeformed flange height ($(d_f-d_0)/2$) and l_f the deformed flange height. The flange elongation simulated is also depicted in Table 3.

5. Conclusions

In this work a successful numerical model of the single stage hole-flanging process by SPIF has been carried out using ANSYS. The analysis of the numerical strain paths on the formed sheet within the Forming Limit Diagram (FLD) allows predicting the failure or success of the flanged parts for the different pre-cut holes. For the cases here analyzed, the predictions agree reasonably well with experimental data. Additionally, the limiting forming ratio and the flange elongations have also been obtained and satisfactorily compared with the experimental results. Having precise numerical models is crucial to analyze in detail variables that cannot be quantified in practice, such as the stresses or the strains throughout the sheet thickness, as a first step to an efficient optimization of the forming process.

Acknowledgements

The authors wish to thank the Spanish Government for its financial support through the research project DPI2015-64047-R.

References

[1] F. Stachowicz, Arch. Civil Mech. Eng. 8 (2) (2008) 167–172.
[2] J. Jeswiet, F. Micari, G. Hirt, A. Bramley, J. Duflou, J. Allwood, CIRP Annals – Manuf. Technol. 54 (2) (2005) 88–114.
[3] G. Centeno, M.B. Silva, V.A.M. Cristino, C. Vallellano, P.A.F Martins, Int. J. Mach. Tools Manuf. 59 (2012) 46–54.
[4] Z. Cui, L. Gao, CIRP J. Manuf. Sc. Technol. 2 (2010) 124–128.
[5] L. Montanari, V.A. Cristino, M.B. Silva, P.A.F. Martins, Int. J. Adv. Manuf. Technol. 69 (5) (2013) 1175–1183.
[6] A. Petek, K. Kuzman, R. Fijavž, Key Eng. Materials 473 (2011) 105-112.
[7] M. Borrego, D. Morales-Palma, A.J. Martínez-Donaire, G. Centeno, C. Vallellano, J. Mater. Process. Tech. 237 (2016) 320–330.
[8] M. Borrego, D. Morales-Palma, A.J. Martínez-Donaire, G. Centeno, C. Vallellano, Proc. Engng. 135 (2015) 290-297.
[9] F. Barlat, K. Lian, Int. Journal of Plasticity 5 (1) (1989) 51–66.
[10] A.J. Martínez-Donaire, F.J. García-Lomas, C. Vallellano, Mater. Des. 57 (2014) 135–145.
[11] A. Caballero, Master Thesis, Univ. of Seville (2015), supervisor: A.J. Martínez-Donaire.